International Journal of Chemical, Materials and Biomolecular Sciences
ISSN: 2415-6620
Vol:5, No:8, 2011

Experimental Design and Performance Analysis in Plasma Arc Surface Hardening

M.I.S. Ismail and Z. Taha

***Abstract*—**In this paper, the experimental design of using the Taguchi method is employed to optimize the processing parameters in the plasma arc surface hardening process. The processing parameters evaluated are arc current, scanning velocity and carbon content of steel. In addition, other significant effects such as the relation between processing parameters are also investigated. An orthogonal array, signal-to-noise (S/N) ratio and analysis of variance (ANOVA) are employed to investigate the effects of these processing parameters. Through this study, not only the hardened depth increased and surface roughness improved, but also the parameters that significantly affect the hardening performance are identified. Experimental results are provided to verify the effectiveness of this approach.

***Keywords*—**Plasma arc, hardened depth, surface roughness, Taguchi method, optimization.

I. Introduction

THE method of surface hardening of steels and alloys with the heat source are widely used a concentrated energy flow such as laser beam, electron beam, or plasma arc [1]. The surface hardening method is a modification of the surface structure of steel containing sufficient carbon to allow the transformation from austenite to martensite after the appropriate amount of heat is applied to the surface followed by rapid cooling of the heated layer by heat sink. .

The surface hardening process has been typically carried out by laser beam [2], [3] and electron beam [4], [5]. However, there is very little independent published information available on the use of plasma arc source for surface hardening [6]. As a heat source, a plasma arc possesses advantages over electron beams or lasers. Plasma arc does not require vacuum chamber as in the case of electron beam, or a complex and expensive optical-mechanical system for laser. In fact, the plasma arc is widely used for welding [7], cutting [8] and forming [9], as well as in surface modification of biomedical materials [10]. Therefore, the plasma arc process is one of the most attractive methods.

Plasma arc surface hardening is a promising technology in manufacturing, such as in the automobile and metal working industries. The rapidity, flexibility and lower cost of the method, can improve the competitiveness of these industries. This technology began in 1980s, and from that time until now, the development of plasma arc surface hardening technology was more concentrated on the experimental studies [1], [6], [11]–[15]. Most of the studies have been developed by using trial and error or empirical methods. Classical experimental design methods are too complex and are not easy to use. A large number of experiments have to be carried out when the number of the process parameters increases. This also proves to be expensive and time consuming.

The objective of the experimental design is to optimize the settings of the parameter values. The Taguchi method is a powerful, high-quality experimental tool [16], [17]. Using a simple, effective and systematic approach, the optimal process parameters can be derived. Taguchi method uses a special design called orthogonal array to study the entire parameter space with a small number of experiments. In this method, process parameters which influence the processes are separated into two main groups: control factors and noise factors [16]. A statistical analysis of variance (ANOVA) is performed to identify the process parameters that are statistically significant. The optimal combination of the process parameters can then be predicted based on the above analysis.

In this study, the effects of the processing parameters and their significance on the hardened depth and surface roughness are statistically evaluated using ANOVA. Also, an optimization study for combination of processing parameters to achieve high hardened depth and low surface roughness is investigated. Experiments were conducted using different processing parameters, namely, arc current, scanning velocity and carbon content of steel. The settings of processing parameters were determined by using Taguchi experimental design method.

II. Experimental Work

The experimental studies were performed on a plasma arc machine with torch diameter of 1.6 mm, which integrated with a six degree-of-freedom articulated robot. The negative terminal of the power supply is connected to tungsten electrode and the workpiece is connected to the positive terminal of the power source as shown in Figure 1. Argon gas was used at 6 bar as shielding gas to minimize oxidation. The nozzle–workpiece standoff distance was kept constant at 13 mm. The selected currents of plasma arc were 30 A and 60 A. The scanning velocities of plasma arc were 0.1 m/s and 0.3 m/s. ASSAB 618 and ASSAB DF3 steels with carbon content of 0.38 wt.% and 0.90 wt.% were used in this study, respectively. The chemical compositions of both tool steels are shown in Table 1.

M.I.S. Ismail is with the Department of Mechanical and Manufacturing Engineering, Faculty of Engineering, Universiti Putra Malaysia, 43400 Serdang, Selangor, Malaysia (corresponding author; e-mail: ms_idris@eng.upm.edu.my).

Z. Taha was with Universiti Malaya, Malaysia. He is now with the Universiti Malaysia Pahang, 26300 Kuantan, Pahang, Malaysia (e-mail: zaharitaha@ump.edu.my).

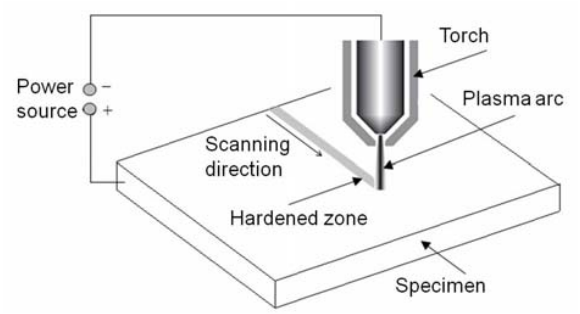

Fig. 1 Schematic diagram of experimental setup

TABLE I
CHEMICAL COMPOSITION OF THE MATERIAL USED

Material	C	Mn	Cr	Si	Mo	Ni	W
ASSAB 618	0.38	1.50	1.90	0.30	0.15	1.00	-
ASSAB DF3	0.90	1.20	0.85	-	-	-	0.55

Unit: wt.%

Specimens of size 60 x 40 x 10 mm^3 were cut from a thick plate, ground and polished with silicon carbide paper in order to remove oxides and obtain a smooth surface. After scanning the steel surface with different conditions, the surface roughness of each track were measured at three different positions along the track length using a Mahr Perthometer M1 tester. Subsequently, the hardened specimens were cut perpendicular to the scanning direction, ground, polished and etched in 2 % Nital for hardened depth measurements using an optical microscope.

In order to ensure the surface hardening has produced hardened layer, the microstructure and hardness distribution of the hardened zones were investigated. A typical transverse section of a plasma arc hardened specimen is shown in Figure 2, which depicts the characteristics zones that form below the surface of the material. It shows the profile of a hardened zone which can be regarded as semi-spherical in shape, with the maximal hardened depth in the central zone of the plasma arc track. Figure 3(a) shows the microstructure at the top surface area of the ASSAB 618 specimens was found to consist of lath martensite. It is clear as shown in Figure 3(b), the phase transformed to martensite as well as a small amount of retained austenite on the top surface of the ASSAB DF3 specimens. The presence of retained austenite is a result of increased carbon content. This untransformed austenite occurs owing to the martensite transformation finish temperature (M_f) dropping below room temperature, resulting in a lower hardness in the hardened zone.

Processing parameters of plasma arc influence the hardness distribution of the hardened zones. Figure 4(a) and 4(b) shows the relationship between hardness distribution and distance from the top surface after plasma arc surface hardened of ASSAB 618 and ASSAB DF3 with each arc current and scanning velocity setting, respectively. In the hardness curves, at increasing depths, three zones with different hardness can be noted. The first zone has a gradual decrease of the hardness occurred within the zone, in the second zone, these hardness values decrease sharply, while the third zone the hardness gradually falls down to its original hardness value of the base material. The maximum hardness of the hardened zone indicated was 849 HV.

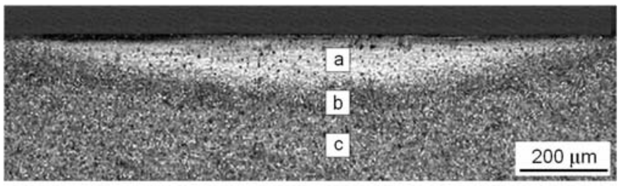

Fig. 2 Transverse section of a plasma arc hardened specimen showing the (a) hardened zone, (b) heat-affected zone and (c) base metal

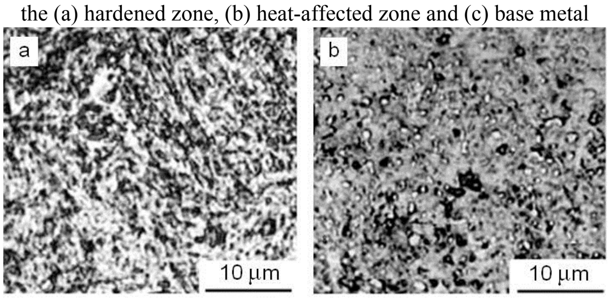

Fig. 3 Optical micrographs of the hardened zones (a) ASSAB 618 and (b) ASSAB DF3

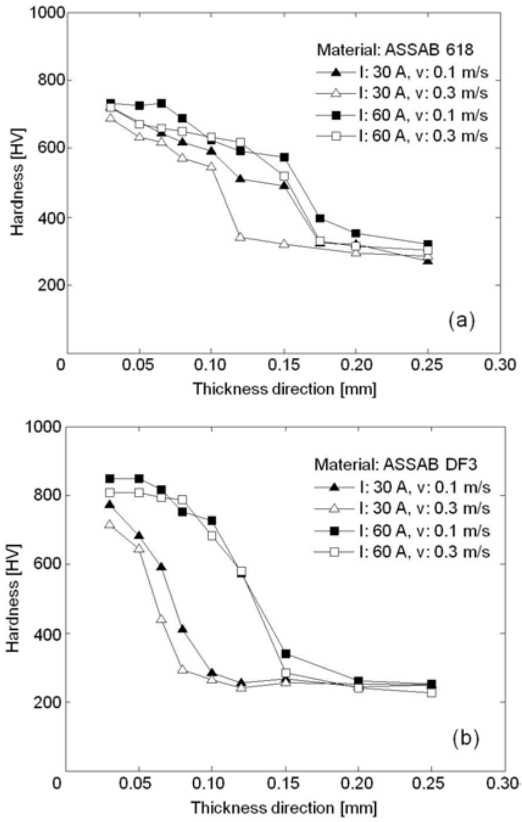

Fig. 4 Hardness profiles of plasma arc surface hardening on (a) ASSAB 618 and (b) ASSAB DF3

III. Experimental Design

In this study, Taguchi method, a powerful method for parameter design of performance characteristics was used to determine optimal processing parameters for maximum hardened depth and minimum surface roughness in plasma arc surface hardening. The three processing parameters, namely arc current (A), scanning velocity (B) and carbon content (C) were used as control factors and each parameter was designed to have two levels as shown in Table 2. Besides the influences of control factors, the influences of their interactions on hardening performances of the hardened specimen were studied as well to check for any confounding of the factors. The influences of interaction of interest were between:

- Arc current and scanning velocity (AxB),
- Arc current and carbon content (AxC),
- Scanning velocity and carbon content (BxC).

In the present study, there are six degrees of freedom regarding the number and levels of control factors and the number of the desired interactions between control factors. A standard Taguchi experimental plan with notation L8(2^3) was chosen. An orthogonal array with arranged control factors is shown in Table 3, where 1 and 2 mean the first level and the second level of each control factor, respectively. The L8 orthogonal array with six columns and eight rows was used. This array has seven degrees of freedom and it can handle two-level process parameters. Each processing parameter is assigned to a column, eight hardening parameter combinations being available. Therefore only eight experiments are required to study the entire processing parameter space when the L8 orthogonal array is used.

The characteristics that higher value represents better hardening performance, such as hardened depth, is called 'higher is better, HB'. Inversely, the characteristics that lower value represents better hardening performance, such as surface roughness, is called 'lower is better, LB'. In quality engineering [16], the S/N ratio (signal-to-noise ratio) could be an effective representation to find the significant parameter from those controlling hardening process parameters by evaluating the minimum variance. Based on the Taguchi method, the S/N calculations of HB and LB are shown in the following equations:

$$\text{HB}: \quad \eta = -10 \cdot \log\left[\frac{1}{n}\sum_{i=1}^{n}\frac{1}{y_i^{\,2}}\right] \tag{1}$$

$$\text{LB}: \quad \eta = -10 \cdot \log\left[\frac{1}{n}\sum_{i=1}^{n} y_i^{\,2}\right] \tag{2}$$

where η denotes the S/N ratio calculated from observed values (unit: dB), y_i represents the experimental observed value of the ith experiment, and n is the number of times each experiment is repeated. Each L8 and measurement of the hardened depth and surface roughness are repeated three times.

The analysis of variance (ANOVA) is applied in order to investigate the process parameters (factors) that significantly affect the quality characteristic. The results of ANOVA are presented in a table that displays for each factor or interaction the value of:

- SS: sum of squared deviations from the mean. For n values of y_i and the mean value $\bar{y}$.

$$\text{SS} = \sum_{i=1}^{n}\left(y_i - \bar{y}\right)^2 \tag{3}$$

- d.f.: degree of freedom which is number of levels for each factor minus 1.
- MS: mean of squares.

$$\text{MS} = \frac{\text{SS}}{\text{d.f.}} \tag{4}$$

- F: F-value is the ratio between the mean of squares effect and the mean of squares error.

$$\text{F} = \frac{\text{MS}_{\text{effect}}}{\text{MS}_{\text{error}}} \tag{5}$$

F-test is used to see the significance of each factor or interaction on the response variable or S/N ratio.

TABLE II
Processing Parameters and Their Levels

Symbol	Parameters	Unit	Level 1	Level 2
A	Arc current	A	30	60
B	Scanning velocity	m/s	0.1	0.3
C	Carbon content	wt.%	0.38	0.90

TABLE III
Experimental Layout Using L8 Orthogonal Array

Experiment number	Factors and interactions					
	A	B	A x B	C	A x C	B x C
1	1	1	1	1	1	1
2	1	1	1	2	2	2
3	1	2	2	1	1	2
4	1	2	2	2	2	1
5	2	1	2	1	2	1
6	2	1	2	2	1	2
7	2	2	1	1	2	2
8	2	2	1	2	1	1

IV. Analysis of Experimental Results

Results of the hardening experiments are studied using the S/N and ANOVA analyzes. Based on the results of the S/N and ANOVA analyzes, optimal settings of the processing parameters for hardened depth and surface roughness are obtained and verified.

A. Analysis of S/N Ratio

According to the equation (1) and (2) above, the S/N ratio of hardening performance for each experiment of L8 can be calculated. Each measurement of the hardened depth and surface roughness were repeated three times and the S/N ratio are computed as can be seen from Table 4 and 5, respectively.

In order to obtain the effects of processing parameters on the hardening performance for each different level, the S/N ratio of each fixed parameters and level for each processing parameters are summed up. From Table 4, taking scanning velocity (B) on hardened depth as an example, the S/N ratio of two levels can be summarized as follows:

$$\text{Level } 1_B = \tfrac{1}{4}(\eta_1 + \eta_2 + \eta_5 + \eta_6) = -15.6672 \quad (6)$$

$$\text{Level } 2_B = \tfrac{1}{4}(\eta_3 + \eta_4 + \eta_7 + \eta_8) = -18.0074 \quad (7)$$

$$\text{Difference}_B = |\text{Level } 1_B - \text{Level } 2_B| = 2.3402 \quad (8)$$

Similarly, those S/N ratios of the other parameters and their interactions on hardened depth and surface roughness are evaluated and given in Table 6 and 7, respectively. The processing parameter with the strongest influence is determined by different values [18]. The higher the difference, the more influential is the processing parameter or an interaction of two processing parameters.

The influence of each processing parameter can be clearly presented with response graphs. A response graph shows the change of the S/N ratio when the setting of the processing parameter is changed from one level to the other. The slope of the line determines the power of the influence of a processing parameter. Response graphs for all processing parameters of the plasma arc surface hardening process on hardened depth is shown in Figure 5. The relative slope of the response graphs indicates that the arc current and carbon content are the most significant factors of hardened depth. It is followed by scanning velocity. This agrees to the S/N response table in Table 6. Figure 6 shows the response graphs of processing parameters on surface roughness. The relative slope of the graphs indicates significance of the parameters. Here, the slope of the graph showing the influence of arc current on surface roughness is greater compared to other graphs. Hence, arc current is the most significant parameter, followed by carbon content and scanning velocity.

The interaction graph between the processing parameters on hardened depth and surface roughness are presented in Figure 7 and Figure 8, respectively. The interpretation is determined by the parallelism of the plotted lines. If the lines are parallel or almost parallel, this indicates there is no meaningful interaction taking place between the plotted factors. The greater the skew between the lines, the greater the strength of the interaction between the factors. Figure 7 shows that the lines are almost parallel for interaction AxB and interaction BxC on hardened depth, which indicate that there is little connection between factors. Whilst, there is a slight angle between the two lines for interaction AxC, which indicates a strong connection is present between factor A and C. Furthermore, the interactions between processing parameters on surface roughness as given in Figure 8 shows that all interactions AxB, AxC and BxC are have a weak influence between each other. However, the relative

TABLE IV
HARDENED DEPTH WITH CALCULATED S/N RATIO

Experiment number	Measured hardened depth, *d* (mm)			S/N ratio
	d_1	d_2	d_3	η (dB)
1	0.1975	0.2050	0.1900	-14.1012
2	0.0950	0.1050	0.1025	-19.9518
3	0.1350	0.1150	0.1475	-17.6950
4	0.0750	0.0800	0.0850	-21.9722
5	0.2100	0.2150	0.2025	-13.5981
6	0.1800	0.1775	0.1750	-15.0178
7	0.1650	0.1725	0.1625	-15.5713
8	0.1475	0.1375	0.1500	-16.7913

TABLE V
SURFACE ROUGHNESS WITH CALCULATED S/N RATIO

Experiment number	Measured hardened depth, *Ra* (mm)			S/N ratio
	Ra_1	Ra_2	Ra_3	η (dB)
1	0.416	0.481	0.448	6.9528
2	0.286	0.236	0.257	11.6847
3	0.348	0.299	0.316	9.8525
4	0.254	0.234	0.249	12.1879
5	0.774	0.729	0.740	2.5230
6	0.552	0.562	0.569	5.0201
7	0.508	0.514	0.589	5.3801
8	0.390	0.449	0.461	7.2413

TABLE VI
S/N RESPONSE TABLE FOR HARDENED DEPTH

Parameters	Level 1 (dB)	Level 2 (dB)	Difference (dB)
A	-18.4300	-15.2446	3.1854
B	-15.6672	-18.0074	2.3402
AxB	-16.6039	-17.0708	0.4669
C	-15.2414	-18.4333	3.1919
AxC	-15.9013	-17.7733	1.8721
BxC	-16.6157	-17.0590	0.4433

Overall mean = -16.8373 dB

TABLE VII
S/N RESPONSE TABLE FOR SURFACE ROUGHNESS

Parameters	Level 1 (dB)	Level 2 (dB)	Difference (dB)
A	10.1695	5.0411	5.1283
B	6.5451	8.6655	2.1203
AxB	7.8147	7.3959	0.4189
C	6.1771	9.0335	2.8564
AxC	7.2667	7.9439	0.6772
BxC	7.2263	7.9844	0.7581

Overall mean = 7.6053 dB

importance amongst the processing parameters for hardened depth and surface roughness still needs to be known so that optimal combinations of the processing parameter levels can be determined more accurately. This will be discussed in the next section using the analysis of variance.

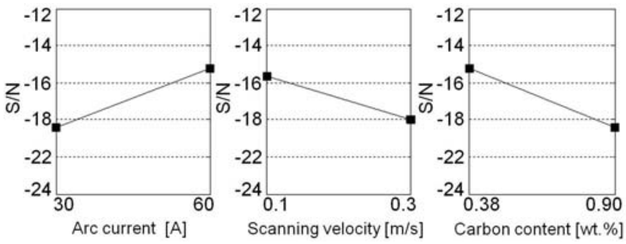

Fig. 5 S/N response graphs for hardened depth

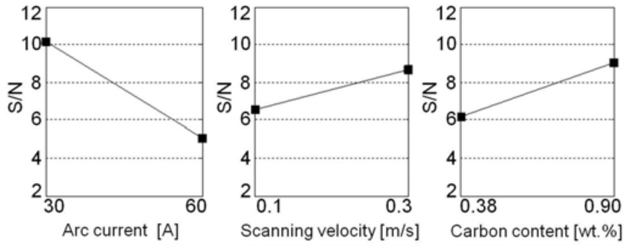

Fig. 6 S/N response graphs for surface roughness

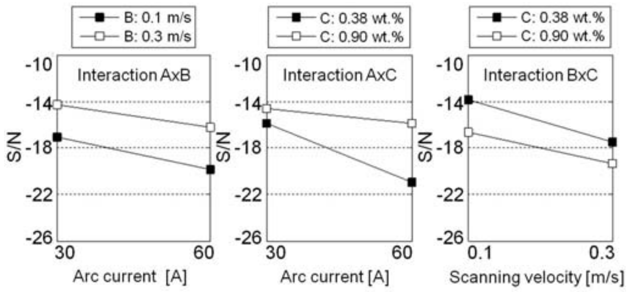

Fig. 7 Interaction graph for hardened depth

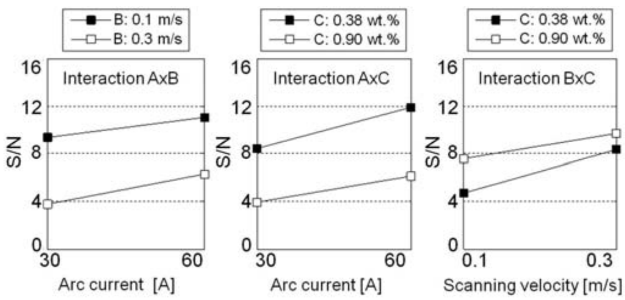

Fig. 8 Interaction graph for surface roughness

B. Analysis of Variance

Using pooling up technique, the insignificant factors and interactions are pooled up with the error and the result of ANOVA for hardened depth is given in Table 8. Statistically, F-test provides a decision at some confidence level as to whether these estimates are significantly different [16]. Larger F-value indicates that the variation of the process parameter makes a big change on the performance characteristics. F-values of the process parameters are compared with the appropriate confidence table. When the F-value of the process parameter is bigger than $F_{\alpha,v1,v2}$-value of the confidence table, where α is risk, $v1$ and $v2$ are degrees of freedom associated with numerator (factor or interaction) and denominator (error).

The factor or interaction for hardened depth is significant with 99 % confidence if F-value exceeds 34.1, and with 95 % confidence for F-value higher than 10.1 [16]. It is evident from the table that the significance of the processing parameters prevails in the following order of importance: (1) carbon content; (2) arc current; (3) scanning velocity, based on the F-value and percentage contribution. Therefore, based on the S/N and ANOVA analyzes, the optimal processing parameters for hardened depth are the arc current at level 2, the scanning velocity at level 1, and the carbon content at level 1. Among the interactions, arc current versus carbon content (AxC) shows significance. All other interactions have an insignificant effect on hardened depth. Since the interaction AxC is significant, Park [19] has recommended interaction AxC table to select their levels as shown in Table 9. It shows the optimum combination for factors A and C is A_2C_1 which shows that the best level of the corresponding factors are same as the optimum levels obtained individually.

Table 10 shows the result of ANOVA for surface roughness. All interactions have an insignificant effect on surface roughness. The factor for surface roughness is significant with

TABLE VIII
ANOVA FOR HARDENED DEPTH

Factors and interactions	SS	d.f.	MS	F	Contribution (%)
A	20.2939	1	20.2939	57.1815 [b]	34.40
B	10.9535	1	10.9535	30.8634 [a]	18.57
C	20.3760	1	20.3760	57.4129 [b]	34.54
AxC	7.0092	1	7.0092	19.7497 [a]	11.88
Pooled error	1.0647	3	0.3549		0.60
Total	59.6973	7			100.00

[a] At least 95 % confidence ($F_{.05,1,3}$ = 10.1)
[b] At least 99 % confidence ($F_{.01,1,3}$ = 34.1)

TABLE IX
INTERACTION BREAKUP OF INTERACTION AXC FOR HARDENED DEPTH

	C_1	C_2	Total
A_1	$\eta_1+\eta_3$ =-15.8981	$\eta_2+\eta_4$ =-20.9620	-36.8601
A_2	$\eta_5+\eta_7$ =-14.5847	$\eta_6+\eta_8$ =-15.9045	-30.4892
Total	-30.4828	-36.8665	-67.3493

TABLE X
ANOVA FOR SURFACE ROUGHNESS

Factors and interactions	SS	d.f.	MS	F	Contribution (%)
A	52.5999	1	52.5999	75.0052 [b]	66.91
B	8.9916	1	8.9916	12.8217 [a]	11.44
C	16.3179	1	16.3179	23.2687 [b]	20.76
Pooled error	2.8051	4	0.7013		0.89
Total	80.7146	7			100.00

[a] At least 95 % confidence ($F_{.05,1,4} = 7.71$)
[b] At least 99 % confidence ($F_{.01,1,4} = 21.2$)

99 % confidence if F-value exceeds 21.2, and with 95 % confidence for F-value higher than 7.71 [16]. The F-values in the ANOVA confirm that the arc current, scanning velocity and carbon content are the significant processing parameters for affecting surface roughness. However, the contribution order of the processing parameters for surface roughness is arc current, then carbon content, and then scanning velocity. This agrees to the plot in Figure 6. The optimal processing parameters for hardened depth are the arc current at level 1, the scanning velocity at level 2, and the carbon content at level 2.

C. Confirmation Experiment

Once the optimal level of the design parameters has been determined, the final step is to predict and verify the improvement of the quality characteristics using the optimal level of the design parameters. The estimated S/N ratio $\hat{\eta}$ using the optimal level of the design parameters can be calculated as:

$$\hat{\eta} = \eta_m + \sum_{i=1}^{o} (\overline{\eta}_i - \eta_m) \quad (9)$$

where η_m is the total mean S/N ratio at the optimal level, and o is the number of the main design parameters that affect the quality characteristics.

The determination of the processing performance at optimal settings of processing parameters from equation (9) can be written with equation (10) and (11). It can derive the expression for hardened depth (equation (12)) and surface roughness (equation (13)) from equation (1) and (2), respectively, and the calculated hardened depth ($\hat{d}$) is 0.2134 mm, and surface roughness ($\hat{Ra}$) is 0.2329 µm at optimal hardening conditions.

$$\begin{aligned}\hat{\eta}_d &= \eta_m + (\overline{A}_2 - \eta_m) + (\overline{B}_1 - \eta_m) + (\overline{C}_1 - \eta_m) \\ &\quad + [(\overline{A}_2\overline{C}_1 - \eta_m) + (\overline{A}_2 - \eta_m) + (\overline{C}_1 - \eta_m)] \\ &= -\eta_m + \overline{B}_1 + \overline{A}_2\overline{C}_1 = 13.4141\end{aligned} \quad (10)$$

$$\begin{aligned}\hat{\eta}_{Ra} &= \eta_m + (\overline{A}_1 - \eta_m) + (\overline{B}_2 - \eta_m) + (\overline{C}_2 - \eta_m) \\ &= -2\eta_m + \overline{A}_1 + \overline{B}_2 + \overline{C}_2 = 12.6579\end{aligned} \quad (11)$$

TABLE XI
CONFIRMATION EXPERIMENT FOR HARDENED DEPTH

	Initial parameter	Optimal parameter	
		Prediction	Experiment
Parameter	A : 30 A	A : 60 A	A : 60 A
	B : 0.2 m/s	B : 0.1 m/s	B : 0.1 m/s
	C : 0.38 wt.%	C : 0.38 wt.%	C : 0.38 wt.%
Level	–	$A_2\,B_1\,C_1$	$A_2\,B_1\,C_1$
Hardened depth (mm)	0.1475	0.2134	0.1975
S/N ratio (dB)	-16.6242	-13.4141	-14.0887

Improvement of S/N ratio = 2.54 dB

TABLE XII
CONFIRMATION EXPERIMENT FOR SURFACE ROUGHNESS

	Initial parameter	Optimal parameter	
		Prediction	Experiment
Parameter	A : 60 A	A : 30 A	A : 30 A
	B : 0.2 m/s	B : 0.3 m/s	B : 0.3 m/s
	C : 0.90 wt.%	C : 0.90 wt.%	C : 0.90 wt.%
Level	–	$A_1\,B_2\,C_2$	$A_1\,B_2\,C_2$
Surface roughness (mm)	0.4793	0.2329	0.2710
S/N ratio (dB)	6.3879	12.6579	11.3406

Improvement of S/N ratio = 4.95 dB

$$\hat{d} = 10^{\hat{\eta}/20} = 10^{-13.4141/20} = 0.2134 \text{ mm} \quad (12)$$

$$\hat{Ra} = 10^{-\hat{\eta}/20} = 10^{-12.6579/20} = 0.2329 \text{ µm} \quad (13)$$

Table XI shows the comparison of the predicted hardened depth with the actual hardened depth using the optimal processing parameters, good agreement between the predicted and actual hardened depth being observed. The increase of the S/N ratio from the initial processing parameters to the optimal processing parameters is 2.54 dB, which means also that the hardened depth is increased by about 1.34 times. Table 12 shows the comparison of the predicted surface roughness with the actual surface roughness using the optimal processing parameters, where a predicted surface roughness consistent with the actual surface roughness is noted. The increase of the S/N ratio from the initial processing parameters to the optimal processing parameters is 4.95 dB and therefore the surface roughness value is improved by about 1.77 times. In other words, the experiment results confirmed the prior design and analysis for enhancing the hardening performance and optimizing the processing parameters. The hardened depth and surface roughness in plasma arc surface hardening processes are greatly improved through the approach.

V. CONCLUSION

In this study, an attempt has been made to investigate the significance of processing parameters and their interactions over the hardening performance, and to determine the optimum level by using Taguchi's design of experiment technique and ANOVA.

The carbon content and arc current are recognized as the most significant factors affecting the hardened depth with contribution rate of 34.54 % and 34.30 %, respectively. The results showed that scanning velocity (18.57 %) was about two times less important than the other parameters for controlling hardened depth. The interaction between arc current and carbon content (AxC) also produces better hardened depth. An optimum parameter combination with the settings of high arc current (60 A), low scanning velocity (0.1 m/s) and low carbon content (0.38 wt.%) of tool steel, i.e. $A_2B_1C_1$ is recommended for the maximum hardened depth.

The surface roughness in plasma arc surface hardening shows that the arc current is most influential factor, which shows a contribution rate of 66.91 %. The second is the carbon content at 20.76 %, and followed by the scanning velocity at 11.44 %. The interactions between processing parameters have shown a very low contribution rate, which can be neglected. In the case of surface roughness, the optimum condition was obtained with the settings of low arc current (30 A), high scanning velocity (0.3 m/s) and high carbon content (0.90 wt.%) of tool steel.

Based on the result of the confirmation experiment, the hardened depth is increased by 1.34 times while the surface roughness is improved by 1.77 times. The experimental results have shown that the hardened depth and surface roughness in plasma arc surface hardening are greatly improved by using this approach.

REFERENCES

[1] V.S. Kraposhin, A.V. Bobrov, and O.S. Gaponenko, "Surface hardening of 9KhF steel by heating with a plasma gun," *Metal Science and Heat Treatment*, vol. 31, no. 11, pp. 816–821, 1989.

[2] J. Ruiz, V. Lopez, and B.J. Fernandez, "Effect of surface laser treatment on the microstructure and wear behaviour of grey iron," *Materials and Design*, vol. 17, no. 5/6, pp. 267–273, 1996.

[3] J.S. Selvan, K. Subramaniam, and A.K. Nath, "Effect of laser surface hardening on En18 (AISI 5135) steel," *Journal of Material Processing Technology*, vol. 91, pp. 29–36, 1999.

[4] J.R. Hwang, and C.P. Fung, "Effect of electron beam surface hardening on fatigue crack growth rate in AISI 4340 steel," *Surface and Coatings Technology*, vol. 80, pp. 271–278, 1996.

[5] R.G. Song, K. Zhang, and G.N. Chen, "Electron beam surface treatment. Part I: Surface hardening of AISI D3 tool steel," *Vacuum*, vol. 69, pp. 513–516, 2003.

[6] E. Bourithis, A. Tazedakis, and G. Papadimitriou, "A study on the surface treatment of Calmax tool steel by a plasma transferred arc (PTA) process," *Journal of Material Processing Technology*, vol. 128, pp. 169–177, 2002.

[7] W. Luo, "The corrosion resistance of 0Cr19Ni9 stainless steel arc welding jonts with and without arc surface melting," *Materials Science and Engineering A*, vol. 345, pp. 1–7, 2003.

[8] J. Wang, K. Kusumoto, and K. Nezu, "Plasma arc cutting torch tracking control," *Science and Technology of Welding and Joining*, vol. 6, no. 3, pp. 154–158, 2001.

[9] C.X. Pan, Y.W. Chen, and A.T. Male, "Microstructural development in plasma jet forming of sheet steels," *Materials Science and Technology*, vol. 18, pp. 1151–1155, 2002.

[10] P.K. Chu, J.Y. Chen, L.P. Wang, and N. Huang, "Plasma surface modification of biomaterials," *Materials Science and Engineering*, vol. 36, pp. 143–206, 2002.

[11] V.A. Linnik, A.K. Onegina, A.I. Andrev, K.K. Aldarkin, V.M. Sinaiskii, and L.P. Grigorenko, "Surface hardening of steel by plasma hardening," *Metalloyed Term Obrab Met.*, vol. 4, pp. 2–5, 1983.

[12] Z. Nitkiewicz, and L. Jeiorski, "Plasma heat treatment of steel: Microstructures, properties and applications," *Materials Science and Engineering*, vol. A140, pp. 474–478, 1991.

[13] S.S. Samotugin, "Plasma treatment of tool steels," *Welding International*, vol. 12, no. 3, pp. 225–228, 1998.

[14] M. Yan, W.Z. Zhu, W. Luo, X.B. Zhang, B.C. Zhou, and X.B. Zhao, "Effect of plasma arc scanning on the wear resistance of gray iron," *Materials Letters*, vol. 56, pp. 14–18, 2002.

[15] W.X. Pan, X. Meng, G. Li, Q.X. Fei, and C.K. Wu, "Feasibility of laminar plasma jet hardening of cast iron surface," *Surface and Coatings Technology*, vol. 197, pp. 345–350, 2005.

[16] P.J. Ross, *Taguchi Techniques for Quality Engineering.* New York: McGraw-Hill, 1996.

[17] G. Taguchi, *Introduction to Quality Engineering.* Tokyo: Asian Productivity Organization, 1986.

[18] J. Kopac, M. Bahor, and M. Sokovic, "Optimal machining parameters for achieving the desired surface roughness in fine turning of cold pre-formed steel workpiece," *International Journal of Machine Tool and Manufacture*, vol. 42, pp. 707–716, 2002.

[19] S.H. Park, *Robust Design and Analysis for Quality Engineering.* London: Chapman and Hall, 1996.